Seismic Spectral Attributes of Apparent Attenuation: Part 1 - Methodology

Fangyu Li, The University of Oklahoma; Huailai Zhou, Chengdu University of Technology;*
Lanbin Li, China University of Geosciences (Wuhan); Kurt J. Marfurt, The University of Oklahoma;

Summary

Ideally, accurate seismic attenuation estimation is extremely useful for reservoir characterization, subtle geological structure identification, and seismic signal compensation. However, seismic attenuation not only distorts their amplitudes but also disperses seismic waves, which gives rise to a number of issues and renders the accurate attenuation estimation impossible. As the measurement of attenuation, the absolute value of quality factor Q does not interest us in seismic interpretation, and the relative value is more important. Instead of struggling to characterize the accurate Q value, we propose a package of seismic spectrum characterization based attenuation attributes to evaluate apparent attenuation effects. The proposed attributes assume the seismic wave is propagating through the earth as a Richer wavelet. Based on this, the attributes' validities are proved analytically in this paper (Part 1: Methodology). Using field data results (presented in the following paper, see Part 2), it is shown that the proposed seismic attenuation attributes are effective and robust for seismic interpretation compared to previous Q estimation results.

Introduction

Like a time-variant low-pass filter, seismic attenuation typically causes the amplitudes of the higher-frequency components to decay more rapidly than those of the lower frequencies (Raikes and White, 1984). Conventionally, energy dissipation properties are described by quality (*Q)* factors attributed to the materials. However, despite their common name and intuitively expected similarity, the Q values encountered in different contexts are not the same (Zhu, 2014; Morozov and Ahmadi, 2015). This apparent attenuation consists of anelastic losses from absorption and elastic losses due to scattering, which results in a seismic wavelet that is more stretched and exponentially smaller in amplitude in time, or depth, with the peak frequency of the data reducing (Reine et al., 2012).

Previous attenuation estimation methods usually just measure the apparent attenuation without classifying its types (Quan and Harris 1997; Zhang and Ulrych 2002; Li et al, 2015). Since the apparent attenuation is a combination of all kinds of seismic attenuation, it is inapproporiate to still call it "*Q* estimation", which should be specific to certain kinds.

As seismic interpreters, we are usually not interested in the absolute Q value, but really care about the relative attenuation effects between a position and its surroundings. We propose a package of seismic attenuation attributes based on Ricker wavelet spectrum assumption. In this paper, all of the attributes are proved to be related to apparent attenuation analytically. A synthetic example is also presented, while some field data examples are in the following paper (Part 2: Application). Formula derivations and application verifications persuade us that the proposed attributes very promising for seismic attenuation interpretation.

Apparent Attenuation on Spectrum

When a seismic wave propagates in a viscoelastic medium in a constant linear frequency attenuation model, the apparent Q arises by considering a traveling wave whose spectral amplitude exponentially reduces with traveltime as (Aki and Richards, 2002)

$$A(\omega,\tau)=S(\omega)\exp\left(-\frac{\omega\tau}{2Q}\right), \tag{1}$$

where, $S(\omega)$ is the source wavelet spectrum, τ is the travel time, and $A(\omega,\tau)$ is the received signal spectrum including all geometric spreading, source, and receiver effects. Here, it clearly shows that the apparent Q is not related to certain specific rock properties. It is just a symbol for apparent attenuation in frequency domain. Hence, adopting seismic attributes to characterize this effect is not inapproriate.

The Ricker Wavelet and Its Frequencies

We assume the seismic signal is propagating as a Ricker wavelet, which is suitable for empirical situations. Wang (2015) discussed frequencies of the Ricker wavelet, which inspired some of the following derivations.

The Fourier transform of the Ricker wavelet can be expressed as

$$R(\omega)=\frac{2\omega^2}{\sqrt{\pi}\omega_m^3}\exp\left(-\frac{\omega^2}{\omega_m^2}\right), \tag{2}$$

where ω is the angular frequency and ω_m is the dominant frequency (the most energetic frequency, also in radians per second). This is an amplitude spectrum, so it is real and nonnegative.

Seismic Attenuation Attributes: Methodology

We can set the derivative of the amplitude spectrum to zero to get the corresponding peak frequency ω_p:

$$\frac{\partial R(\omega)}{\partial \omega} = \frac{4\omega}{\sqrt{\pi}\omega_m^3}\left(1-\frac{\omega^2}{\omega_m^2}\right)\exp\left(-\frac{\omega^2}{\omega_m^2}\right) = 0 . \qquad (3)$$

This leads to $\omega_p = \omega_m$.

Combining Equation (1) and (2), we can obtain the peak frequency after attenuation:

$$\frac{\partial\left[R(\omega)\exp\left(-\frac{\omega\tau}{2Q}\right)\right]}{\partial\omega} = \frac{\partial R(\omega)}{\partial\omega}\exp\left(-\frac{\omega\tau}{2Q}\right) - R(\omega)\frac{\tau}{2Q}\exp\left(-\frac{\omega\tau}{2Q}\right) = 0 . \qquad (4)$$

This leads to

$$\tilde{\omega}_p = \frac{\omega_m^{\ 2}}{2}\left(\sqrt{\frac{\tau^2}{4Q^2}+\frac{4}{\omega_m^{\ 2}}}-\frac{\tau}{4Q}\right). \qquad (5)$$

Note that when attenuation is stronger (Q^{-1} is larger), the peak frequency value is smaller.

The peak of the Ricker wavelet amplitude spectrum is

$$R(\omega_p) = \frac{2}{e\sqrt{\pi}\omega_m} . \qquad (6)$$

In the following work, we adopt the normalized Ricker wavelet amplitude spectra. It is obtained by dividing the spectra with its maximum value to unity (Hermana et al. (2013) also adopted this way in attenuation based hydrocarbon prediction). The normalized Ricker wavelet amplitude spectrum is formulated as:

$$\bar{R}(\omega) = \frac{R(\omega)}{R(\omega_p)} = \frac{\frac{2\omega^2}{\sqrt{\pi}\omega_m^3}\exp\left(-\frac{\omega^2}{\omega_m^2}\right)}{\frac{2}{e\sqrt{\pi}\omega_m}} = \frac{\omega^2}{\omega_m^2}\exp\left(1-\frac{\omega^2}{\omega_m^2}\right). \qquad (7)$$

Seismic Attenuation Attributes

Our objective is to propose attributes to measure the spectral changes caused by attenuation. We assume the decrease in peak frequency is the main change, and after attenuation the seismic spectrum is still a Ricker wavelet spectrum. Set the reference spectrum without attenuation to $R_0(\omega)$ with peak frequency ω_{m0}. The received attenuated spectrum is $R_1(\omega)$ with peak frequency ω_{m1}. According to Equation (5), ω_{m1} should be smaller than ω_{m0}, and the difference between reference and received peak frequencies shows the attenuation strength: larger difference, stronger attenuation.

High Order Statics

As is known, the amplitude spectrum of the Ricker wavelet is the Gaussian distribution multiplied by a factor ω^{-2}, and thus is asymmetric and "unGaussian" in the frequency domain. So we can use skewness and kurtosis to measure the spectra's shapes:

$$skewness = \frac{\mu_3}{\sigma^3} = \frac{\mu_3}{\left(\sigma^2\right)^{\frac{3}{2}}} = \frac{\int_0^\infty(\omega-\omega_m)^3\frac{\omega^2}{\omega_m^2}\exp\left(1-\frac{\omega^2}{\omega_m^2}\right)d\omega}{\left(\int_0^\infty(\omega-\omega_m)^2\frac{\omega^2}{\omega_m^2}\exp\left(1-\frac{\omega^2}{\omega_m^2}\right)d\omega\right)^{\frac{3}{2}}} = \frac{\frac{1}{8}e\cdot\omega_m^{\ 4}\cdot\left(20-11\sqrt{\pi}\right)}{\left[\frac{1}{8}e\cdot\omega_m^{\ 3}\cdot\left(-8+5\sqrt{\pi}\right)\right]^{\frac{3}{2}}} \approx \frac{1.0777}{\sqrt{\omega_m}} . \qquad (8)$$

$$kurtosis = \frac{\mu_4}{\sigma^4} = \frac{\mu_4}{\left(\sigma^2\right)^2} = \frac{\int_0^\infty(\omega-\omega_m)^4\frac{\omega^2}{\omega_m^2}\exp\left(1-\frac{\omega^2}{\omega_m^2}\right)d\omega}{\left(\int_0^\infty(\omega-\omega_m)^2\frac{\omega^2}{\omega_m^2}\exp\left(1-\frac{\omega^2}{\omega_m^2}\right)d\omega\right)^2} = \frac{\frac{1}{16}e\cdot\omega_m^{\ 5}\cdot\left(-96+55\sqrt{\pi}\right)}{\left[\frac{1}{8}e\cdot\omega_m^{\ 3}\cdot\left(-8+5\sqrt{\pi}\right)\right]^2} \approx \frac{2.9390}{\omega_m} . \qquad (9)$$

Note the lower peak frequency, the larger skewness, and larger kurtosis. So, we can measure their changes to estimate the relative attenuation.

Spectral Bandwidth

The frequency bandwidth is defined by the frequency components spreading at some proportion of the spectrum peak (maximum value). Here, we set the frequency band to be measured at $\alpha(\alpha<1)$ of the peak, which is 1 in the normalized spectrum, so we get:

$$\bar{R}(\omega) = \frac{\omega^2}{\omega_m^2}\exp\left(1-\frac{\omega^2}{\omega_m^2}\right) = \alpha , \qquad (10)$$

which leads to the inverse exponential equation

$$-\frac{\omega^2}{\omega_m^2}\exp\left(-\frac{\omega^2}{\omega_m^2}\right)=-\frac{\alpha}{e}, \tag{11}$$

with an analytical solution expressed in terms of the Lambert **W** function:

$$-\frac{\omega^2}{\omega_m^2}=\mathrm{W}\left(-\frac{\alpha}{e}\right). \tag{12}$$

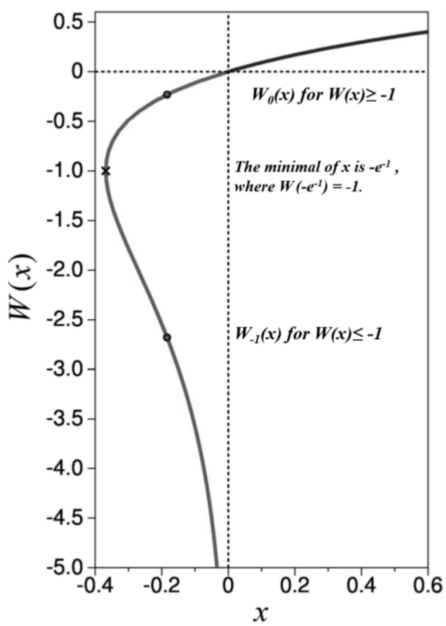

Figure 1: Lambert ***W*** function, modified from Wang (2015).

The solution of an inverse exponential equation $z\exp(z)=x$ is $z=\mathrm{W}(x)$, where W(x) is the Lambert **W** function, displayed in Figure 1. Then the frequency band $[\omega_{low},\omega_{high}]$ is given by

$$\begin{aligned}\omega_{low}&=\omega_m\sqrt{-\mathrm{W}_0\left(-\frac{\alpha}{e}\right)},\\ \omega_{high}&=\omega_m\sqrt{-\mathrm{W}_{-1}\left(-\frac{\alpha}{e}\right)}.\end{aligned} \tag{13}$$

The spectral bandwidth is

$$\omega_b=\omega_m\left(\sqrt{-\mathrm{W}_{-1}\left(-\frac{\alpha}{e}\right)}-\sqrt{-\mathrm{W}_0\left(-\frac{\alpha}{e}\right)}\right). \tag{14}$$

The variable α is fixed in each situation, so the bandwidth in frequency domain is only related to the peak frequency. Thus, after attenuation, the peak frequency will be lower, and the spectral bandwidth will be narrower.

Spectral Slopes

We compute the expressions of spectral slope averages of low frequencies (from $\beta\omega_m$ to ω_m , $\beta<1$) and high frequencies (from ω_m to $\sigma\omega_m$, $\sigma>1$), respectively.

$$\begin{aligned}Slope_{low}&=\frac{\int_{\beta\omega_m}^{\omega_m}\frac{\partial\bar{R}(\omega)}{\partial\omega}d\omega}{(1-\beta)\omega_m}=\frac{\bar{R}(\omega_m)-\bar{R}(\beta\omega_m)}{(1-\beta)\omega_m}\\ &=\frac{\frac{\omega_m^2}{\omega_m^2}\exp\left(1-\frac{\omega_m^2}{\omega_m^2}\right)-\frac{\beta^2\omega_m^2}{\omega_m^2}\exp\left(1-\frac{\beta^2\omega_m^2}{\omega_m^2}\right)}{(1-\beta)\omega_m}\\ &=\frac{1-\beta^2\exp\left(1-\beta^2\right)}{(1-\beta)\omega_m}\end{aligned} \tag{15}$$

$$\begin{aligned}Slope_{high}&=\frac{\int_{\omega_m}^{\sigma\omega_m}\frac{\partial\bar{R}(\omega)}{\partial\omega}d\omega}{(\sigma-1)\omega_m}=\frac{\bar{R}(\sigma\omega_m)-\bar{R}(\omega_m)}{(\sigma-1)\omega_m}\\ &=\frac{\frac{\sigma^2\omega_m^2}{\omega_m^2}\exp\left(1-\frac{\sigma^2\omega_m^2}{\omega_m^2}\right)-\frac{\omega_m^2}{\omega_m^2}\exp\left(1-\frac{\omega_m^2}{\omega_m^2}\right)}{(\sigma-1)\omega_m}\\ &=-\frac{1-\sigma^2\exp\left(1-\sigma^2\right)}{(\sigma-1)\omega_m}\end{aligned} \tag{16}$$

Both of the slopes have a format of Lambert function in Figure 1, so we can estimate their values. The peak frequency and low frequency slope have an inverse relationship. A decrease in peak frequency will indicate an increase in low frequency slope. The low frequency slope is always positive and the high frequency slopes is always negative. The decrease in peak frequency causes the high frequency slope to become more negative but with a larger absolute value.

Energy Reduction

Let's compute the energy difference between normalized reference and received spectra on the whole band, from 0 to infinity:

$$\begin{aligned}ER_{all}&=\int_0^\infty\left[\frac{\omega^2}{\omega_{m0}^2}\exp\left(1-\frac{\omega^2}{\omega_{m0}^2}\right)-\frac{\omega^2}{\omega_{m1}^2}\exp\left(1-\frac{\omega^2}{\omega_{m1}^2}\right)\right]d\omega\\ &=\frac{1}{4}e\sqrt{\pi}\left(\omega_{m0}-\omega_{m1}\right)\end{aligned}. \tag{17}$$

This formula shows that spectral energy will decay after attenuation even they are both normalized, and the stronger attenuation, the larger energy reduction.

$$ER_{high}=\int_{\omega_c}^{\infty}\left(R_0(\omega)-R_1(\omega)\right)d\omega. \tag{18}$$

Seismic Attenuation Attributes: Methodology

Actually, in Equation (18) we can also just compare the spectral energies of higher frequency components, (e.g. Mitchell et al. (1996) proposed a similar energy absorption analysis (EAA) attribute.), starting from their crossover frequency ω_c . As ω_{m1} is smaller, ω_c is smaller, and the differences at frequencies larger than previous ω_c will be larger, so the energy in higher frequencies will reduce more, when the attenuation is stronger.

Synthetic Example

In order to test our proposed attributes, we apply them in a synthetic example. (Field data application can be found in the following paper: Part 2-Application.) Figure 2 shows the normalized spectra of reference and attenuated signal. Note that when attenuation (1/*Q*) is stronger, the peak frequency is smaller, and more high frequency energy attenuated. Figure 3 displays results of attenuation attributes associated with different *Q* values. Because we just want to know the relative attenuation relationship, all values are shown in the normalized way. It is clear that every attributes has a good correspondence with the attenuation factor.

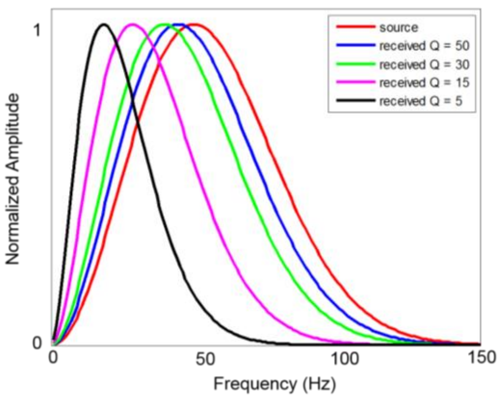

Figure 2: Reference wavelet spectrum and attenuated spectra with different *Q* values.

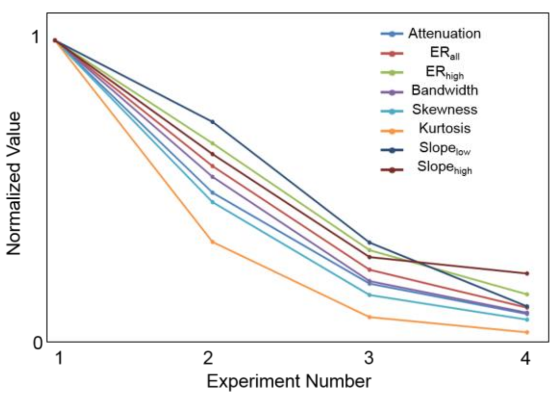

Figure 3: Normalized values of seismic attenuation attributes.

Note that the attenuated wavelets are not exactly Ricker wavelets anymore. But the proposed seismic attenuation attributes are still effective to characterize attenuation effects, as shown in Figure 3.

What's more, in order to suppress noises, we usually just analyze the effective-band (shown in Equation (10)) of the spectrum, and when noise is stronger, the coefficient is larger. Within the effective bands, the actual seismic spectra shows properties described in our derivations. Hence, our approximation is sound and all the proofs are meaningful.

Conclusions

We propose a package of seismic attenuation attributes based on spectral shape changes to characterize apparent seismic attenuation. When the seismic attenuation becomes stronger, the energy reductions in full bands and high frequencies will be larger, the spectral bandwidth will be narrower, skewness and kurtosis will be larger, and the spectral slopes will also have the corresponding changes. All these changes are associated with seismic attenuation non-linearly, but they are promising indicators for relative attenuation changes which are useful for seismic interpreters. The synthetic example proves the relationship between the seismic attributes we propose and the attenuation effects. Field data applications are included in the following paper: Part 2 – Application.

Acknowledgments

We express our gratitude to the industry sponsors of the Attribute-Assisted Seismic Processing and Interpretation (AASPI) Consortium for their financial support. The second author (corresponding author) also appreciates the Chinese Scholarship Council for financial support.